Available online at www.sciencedirect.com
SCIENCE DIRECT®
Journal of Nuclear Materials 344 (2005) 281–284
journal of nuclear materials
www.elsevier.com/locate/jnucmat

High temperature mass spectrometry: Application to the thermodynamic study of the Fe–Zr system

Sylvie Chatain [a,*], Christine Guéneau [a], Christian Chatillon [b]

[a] Commissariat à l'Energie Atomique Saclay, Direction de l'Energie Nucléaire/Département de Physico-Chimie/Service de Chimie Physique/Laboratoire de Modélisation, de Thermodynamique et de Thermochimie/91191 Gif-sur-Yvette cedex, France
[b] Laboratoire de Thermodynamique et Physico-Chimie Métallurgiques (CNRS UMR 5614, UJF/INPG), ENSEEG – Domaine Universitaire, BP 75, 38402 Saint Martin d'Hères cedex, France

Abstract

The high temperature mass spectrometry method is a standard method for the study of chemical equilibria at high temperature. For our studies of complex nuclear materials, the multiple Knudsen cell is the most promising device to perform thermodynamic activity measurements. We illustrate it with some new results obtained about the iron–zirconium system.

1. Introduction

To build thermochemical databases of nuclear materials we use the CALPHAD (CALculation of PHAse Diagram) method which couples phase diagram data and thermodynamic properties of systems [1]. The first step of system assessment consists of a critical analysis of the available experimental data resulting in both a consistent experimental data set and the identification of missing data that should be obtained via further new and pertinent experiments. Among the different experimental facilities, high temperature mass spectrometry is a key method for studying thermodynamic equilibria at high temperature. Here we illustrate this experimental technique with some results obtained for the iron–zirconium system.

The iron–zirconium system is an important system for issues involving nuclear materials. As a low temperature application it is one of the Zircobase [2] binaries for Zircaloy cladding tubes studies. As a high temperature application it belongs to the U–Zr–O–Fe key quaternary system for in-vessel Corium studies [3]. Previous works on this system have been reported [4–10]. Comparing the two most recent phase diagrams published respectively by Jiang et al. (optimized diagram) [11] (Fig. 1(a)) and Stein et al. (experimental work) [12] (Fig. 1(b)) we observe that several discrepancies remain including the possible existence of the $Fe_{23}Zr_6$ compound, the composition range of Fe_2Zr, the room temperature stability of a $FeZr_2$ intermetallic compound and the liquidus curve in the zirconium-rich part. Regarding experimental data in the liquid phase we remark that these data are sparse due to the experimental difficulties related to alloy oxidation and crucible/liquid alloy interaction. In order to improve the thermodynamic description of this binary system other experimental techniques can be used like differential

* Corresponding author. Tel.: +33 1 69 08 65 10; fax: +33 1 69 08 92 21.
E-mail address: schatain@cea.fr (S. Chatain).

0022-3115/$ - see front matter © 2005 Elsevier B.V. All rights reserved.
doi:10.1016/j.jnucmat.2005.04.055

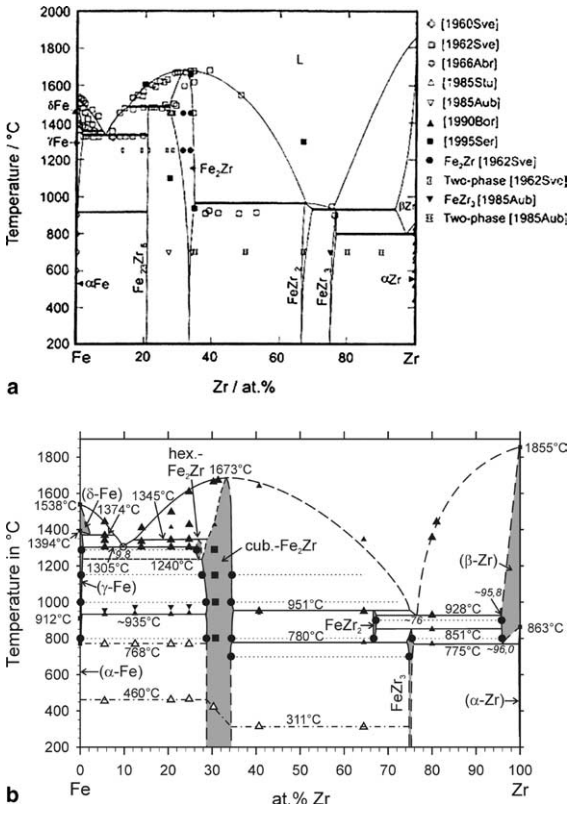

Fig. 1. (a) Fe–Zr phase diagram optimized by Jiang et al. [11] (reproduced with permission from [11] Copyright 2001 ASM). (b) Experimental Fe–Zr phase diagram proposed by Stein et al. [12] according his experimental results (reproduced with permission from [12] Copyright 2002 ASM).

scanning calorimetry (DSC) for phase diagram data, calorimetry for the enthalpy of formation, enthalpy of melting and heat capacity of intermetallic compounds, and finally high temperature mass spectrometry for measuring thermodynamic activity.

2. Experimental method

The thermodynamic activity of iron in iron–zirconium alloys is measured using a well-established high temperature mass spectrometry-Knudsen effusion technique [13–15]. The experimental apparatus is fitted with a multiple cell device as already published [16]. In our experimental conditions, activity determination is readily performed by direct comparison of the iron ionic intensity measured successively in the molecular beams coming from either of the alloy, I_{Fe}, and of pure component as reference, I^0_{Fe} [17,18] cells:

$$a_{Fe} = \frac{I_{Fe}}{I^0_{Fe}}. \quad (1)$$

To improve activity measurements, a restricted collimation has been carried out [19–21].

The multiple effusion device is a block containing four Knudsen effusion cells (Fig. 2), one loaded with pure iron and three others with Fe–Zr alloys, which ensures isothermal conditions. The Knudsen cells are made out of pure ceramic oxides, Al_2O_3 and Y_2O_{3-x} for the reference and Y_2O_{3-x} for the alloys which have exhibited a low chemical reactivity with regard to Fe–Zr liquid alloys.

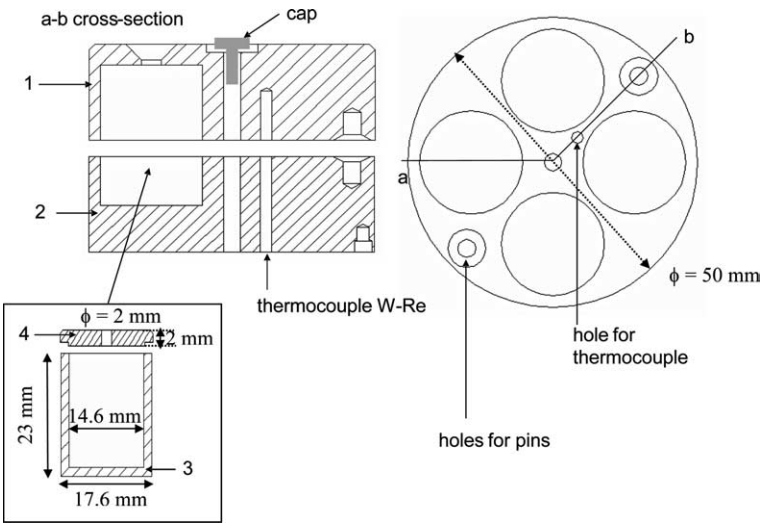

Fig. 2. Multiple cell device fitted with four compartments for the Knudsen effusion cells; 1–2: respectively upper part and lower part of the multiple cell block which is in molybdenum; 3: Knudsen effusion cell in Alumina or Yttria; 4: lid of the cell.

The samples with nominal Zr contents of 50, 60, 67, 75, 78, 85 at.% were elaborated at CEA Saclay (DRT/DCES) from pure Fe (99.9% Optilas) and Zr (Van Arkel) by arc melting under an argon atmosphere in a water-cooled copper crucible. Samples are analysed for oxygen content.

Our technique requires the beam to be in the molecular flow regime which implies that the vapor pressures are less than 10^{-4} bar and the vapor pressures of the components to be high enough to yield measurable ion currents. Iron is much more volatile than zirconium (at $T = 1773$ K, $P^0_{(Fe)} = 1.89$ Pa and $P^0_{(Zr)} = 4.6\times 10^{-6}$ Pa [22]) thus, in our temperature range, it is not possible to measure simultaneously the ionic current of Zr and Fe. For activity determinations, the main mass peak i.e. ^{56}Fe (91.8%) was measured at 15 V ionising potential.

3. Iron activity results

Thermodynamic activities of Fe in the Fe–Zr system were measured for X_{Zr} = 50–85 at.% in the 1503–1843 K temperature range which corresponds essentially to pure solid iron. As shown in Fig. 1, this study includes liquid alloys and several two-phase regions.

Experimental $\ln(a_{Fe})$ data referred to pure iron are presented in Fig. 3 versus $10^4/T$ (K^{-1}). Activity values are referred to γ-solid iron for $T < 1678$ K, to the δ-solid iron in the 1678–1811 K temperature range and to the liquid iron for $T > 1811$ K. Some measurements have been relative to pure liquid iron, but we have not observed a significant change in the slope of the activity curves since the temperature range (1811–1843 K) is small and data are not enough numerous. Due to the small value of $\Delta H^0_{Fe}(\gamma \rightarrow \delta) = 836$ J mol^{-1} [23], the activity referred to γ or δ-solid pure iron is not significantly different.

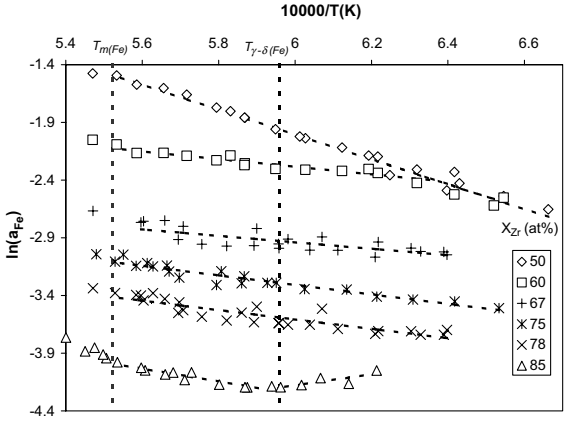

Fig. 3. Natural logarithm of the iron activity experimental data in the Fe–Zr alloy.

Table 1
Natural logarithms of iron activity data $\ln(a_{Fe}) = A + B/T$ with respect to pure solid Fe in the liquid region for alloys

X_{Zr} (at.%)	$\ln(a_{Fe}) = A + B/T$ and temperature range (K)
85	$-(0.9372 \pm 0.3598) - (5530 \pm 628)/T$ (1684–1807)
78	$-(1.1732 \pm 0.2433) - (4058 \pm 411)/T$ (1563–1809)
75	$-(0.8384 \pm 0.1705) - (4116 \pm 289)/T$ (1530–1809)
67	$-(1.2648 \pm 0.3322) - (2791 \pm 581)/T$ (1563–1787)
60	$-(0.3044 \pm 0.2487) - (3299 \pm 425)/T$ (1615–1807)

Table 2
Natural logarithms of iron activity data $\ln(a_{Fe}) = A + B/T$ with respect to pure solid Fe in the two-phase field

X_{Zr} (at.%)	$\ln(a_{Fe}) = A + B/T$
Liquid + β-Zr	$-(7.0413 \pm 1.1828) + (4772 \pm 1945)/T$
Liquid + Fe_2Zr	$(4.4552 \pm 0.2089) - (10767 \pm 340)/T$

For each area, a linear least-mean-square fit is expressed as: $\ln(a_{Fe}) = (A \pm \delta A) + (B \pm \delta B)/T$ (Tables 1 and 2). The average standard deviations in the slope B and the constant coefficient A are calculated using the method proposed by Paule and Mandel [24]. The $\ln(a_{Fe})$ versus $10^4/T$ (K^{-1}) fits are shown in Fig. 3. We observe a break in the curve for two compositions, 60 at.% Zr and 85 at.% Zr which corresponds to the liquidus boundary (liquid + $Fe_2Zr \rightarrow$ liquid or liquid + β-Zr → liquid). Indeed, in the two-phase regions, the activity does only depend on the temperature since the variance equals unity [16] that means that the activity is constant at a given temperature. The liquidus temperature deduced from these fits is respectively (1322 ± 20) °C for X_{Zr} = 60 at.% and (1419 ± 10) °C for X_{Zr} = 85 at.% which is in quite good agreement with other previous experimental values [10,12] and confirm Stein's phase diagram.

4. Conclusion

The multiple Knudsen cell-high temperature mass spectrometry is a powerful tool for studying thermodynamics of condensed phases and vaporization processes. It is also the most promising and direct technique to determine activity in complex systems. The thermodynamic activity of iron in Fe–Zr alloys has been measured for an iron concentration ranging from X_{Zr} = 50–85 at.% and for temperatures ranging from 1503 to 1843 K. The liquidus temperatures for the 60 at.% and 85 at.% were derived from a potentiometric analysis, that is the variation of the natural logarithms of iron activity versus inverse of temperature. These temperature are in quite good agreement the previous data from the literature and confirm Stein's phase diagram.

References

[1] L. Kaufman, H. Bernstein, in: J.L. Margrave (Ed.), Computer Calculation of Phase Diagrams, Academic Press, New York, 1970.

[2] N. Dupin, I. Ansara, C. Servant, C. Toffolon, C. Lemaignan, J.C. Brachet, J. Nucl. Mater. 275 (1999) 287.

[3] C. Guéneau, V. Dauvois, P. Pérodeaud, C. Gonella, O. Dugne, J. Nucl. Mater. 254 (1998) 158.

[4] V.N. Svechnikov, A.T. Spektor, Proc. Acad. Sci. USSR, Chem. Sect. 142 (1962) 231 (tr: Dokl. Akad. Nauk SSSR 143 (1962) 613).

[5] T.O. Malakhova, A.N. Kobylkin, Russ. Metall. 1982 (2) (1982) 187 (tr: Izv. Akad. Nauk SSSR Metall. 1982(2) 205).

[6] D. Arias, J.P. Abriata, Bull. Alloy Phase Diagrams 9 (1988) 597.

[7] Z.M. Alekseeva, N.V. Korotkova, Russ. Metall. 1989 (4) (1989) 197 (tr: Izv. Akad. Nauk SSSR Metall. 1989(4) 202).

[8] H. Okamoto, J. Phase Equilib. 14 (1993) 652.

[9] A.D. Pelton, L. Leibowitz, R.A. Blomquist, J. Nucl. Mater. 201 (1993) 218.

[10] C. Servant, C. Guéneau, I. Ansara, J. Alloys Compd. 220 (1995) 19.

[11] M. Jiang, K. Oikawa, T. Ikeshoji, L. Wulff, K. Ishida, J. Phase Equilib. 22 (2001) 406.

[12] F. Stein, G. Sauthoff, M. Palm, J. Phase Equilib. 23 (2002) 480.

[13] M.G. Inghram, J. Drowart, in: Proceedings of an International Symposium on High Temperature Technology, Asilonar, CA, 6–9 October 1959, McGraw-Hill, New York, 1960, p. 219.

[14] J. Drowart, in: E. Rutner, P. Goldfinger, J.P. Hirth (Eds.), Condensation and Evaporation of Solids, Gordon and Breach, New York, 1964, p. 255.

[15] R.T. Grimley, in: J.L. Margrave (Ed.), The Characterization of High-temperature Vapors, Wiley, New York, 1967, p. 195.

[16] P. Gardie, G. Bordier, J.J. Poupeau, J. Le Ny, J. Nucl. Mater. 189 (1992) 85.

[17] C. Chatillon, A. Pattoret, J. Drowart, High Temp. High Press. 7 (1975) 119.

[18] E. Kato, J. Mass Spectrom. Soc. Jpn. 41 (1993) 297.

[19] M. Baïchi, C. Chatillon, C. Guéneau, S. Chatain, J. Nucl. Mater. 294 (2001) 84.

[20] P. Morland, C. Chatillon, P. Rocabois, High Temp. Mater. Sci. 37 (1997) 167.

[21] M. Heyrman, C. Chatillon, H. Collas, J.L. Chemin, Rapid Commun. Mass Spectrom. 18 (2004) 163.

[22] C.B. Alcock, V.P. Itkin, M.K. Horrigan, Vapor pressure equations of the metallic elements 298–2000 K, Department of Metallurgy and Materials Science, University of Toronto.

[23] L.B. Pankratz, Thermodynamic properties of elements and oxides, United States Department of Interior, Bureau of Mines, 1982.

[24] R.C. Paule, J. Mandel, Pure Appl. Chem. 31 (1972) 371.